



**Joint ICTP-IAEA International School on Radioactive Waste Package Performance Testing |  
(SMR 3636)**

02 Nov 2021 - 22 Nov 2021  
Virtual

---

**T01 - ADIAHA Monday Sunday**

Repackaging and treatment of Soil degradation using Uranium extract-Urea mixed: A strategy for Meeting SDG Two and Six

**T02 - DESAI Ramesh Jayantilal**

SINGLE FORMULA FOR VOLUME

**T03 - GOLGOUN Seyedmohammad - didn't present**

Combined detector model for the purpose of liquid nucleonic density measurement

**T04 - GUEMBOU SHOUOP Sebastien Joel**

Application of Monte Carlo simulations to waste management: projection for the DSRs management in low income countries

**T05 - HUSSAIN Mazhar**

Standardization of Nuclear Data for the Production of Medical Radionuclides

**T06 - JENEBRIE Temesgen Fentahun - didn't present**

Application Radiation

**T07 - MOUSSA HASSANE Ayouba**

Advanced Fuel Cycle Technique Development

**T08 - PENG Haibo**

Macroscopic and microscopic changes in borosilicate glasses after irradiation.

**T09 - SAURAV Suman**

Radioactive waste management for different state of radioactive waste

**T10 - SOW Malick**

Screening Constant by Unit Nuclear Charge Applications to the  $3s^2 3p^5 (2,1,0,3)$ ,  $3s^2 3p^3 (1,1)$  and  $3s^2 3p^3 (3,2,1,3)$  Rydberg Series of  $Ca^{3+}$  Ion

# Repackaging and treatment of Soil degradation using Uranium extract-Urea mixed: A strategy for Meeting SDG Two and Six

Repackaging, treatment, and reuse of radiative materials has been found to have a high potential for the sustainability of the food system. Application of radiatively viable material could trigger soil radiation and influence crop growth and play a role in soil functionality as observed at various stage of maize growth and development in this study

## **SINGLE FORMULA FOR VOLUME**

**RAMESH DESAI**

**MEDICAL CYCLOTRON FACILITY, IMT MANESAR, GURGAON,INDIA**

An exact single equation is derived first time to find the volume of any regular shape (ellipse, sphere, cone etc.) object.

- This equation is simple to remember and so saves one from having to remember a separate equation for every separate regular shape figure
- It also avoids having to use lengthy integral calculus used in modern mathematics
- The equation will be useful in all branches of sciences.

1. Introduction

Industrial radiometric gauge is a device that could be installed on a pipe to measure, monitor, and control liquids in harsh working environments. The first commercial nuclear density gauge was devised in 1971 (Johansen and Jackson, 2004). In this study, we aimed at reducing the error of  $\gamma$ -ray densitometry by using a new technique. The main purpose of this method, combined detector model (CDM), was to calculate the buildup coefficient on-line, and then reduce this effect automatically, which means on-line buildup reduction.

2. Theoretical background

Each nuclear densitometer consists of a radioactive source, detector, and related electronics. The radioactive source emits radiation that could penetrate the vessel, interact with the process material in the pipe (for instance gasoline), and reach the detector (He and Bai, 2014; Hasan and Lucas, 2011; Thorn et al., 1997). The electronics calculates and corrects measuring algorithms (Knoll, 2000; Tan and Fwa, 1991; Sowerby and Rogers, 2005). The radiation intensity is attenuated by the material between the radioactive source and the detector. This principle can be used to measure the density of materials of interest, while a gamma- or X-ray photon detector is used to measure this attenuation. There are two major methods to measure the required parameters (IAEA, 2005): (1) transmission and (2) backscatter method. As showing in Fig. 1, we combined these two methods and tried to extract new equation for nuclear densitometry.

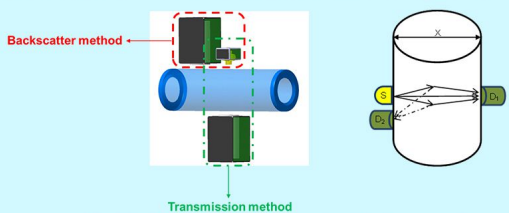


Fig. 1. Schematic view of combination of backscatter and transmission method

2.1. Gamma-ray density measurement

Computational work for the new configuration is mainly based on the transmission method. Backscatter method would help to decline the transmission error and improve the linearity of the model's response (Golgoun et al., 2015). A well-known equation, regardless of buildup factor effect, for transmission method is (Knoll, 2000):

$$I_t = I_0 e^{-\mu \rho x} \quad (1)$$

where  
 $I_t$  = transmitted radiation intensity,  
 $I_0$  = intensity measured when no material is present,  
 $\mu$  = total mass absorption coefficient of material,  
 $\rho$  = density of material, and  
 $x$  = thickness (distance between source and detector).

Considering <sup>137</sup>Cs for this study and according some true assumptions, conventional nuclear density meter formula is as the following:

$$\rho = C_1 \ln(I_t) + C_2 \quad (2)$$

Therefore, the detected radiation intensity " $I_t$ " is only a function of process material's density " $\rho$ ".

2.2. Klein-Nishina compensation coefficient

Klein-Nishina compensation coefficient is the ratio of the probability of forward scattering to the probability of backward scattering (parameters of this calculation can be found in Fig. 2):

$$C_{KN} = \left( \frac{\text{Probability of forward scatter}}{\text{Probability of backscatter}} \right) \quad (3)$$

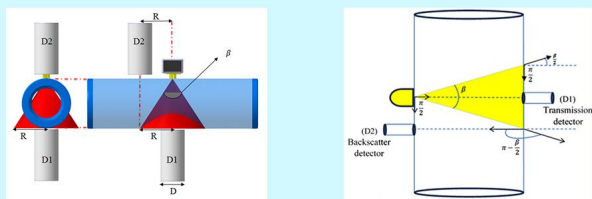


Fig. 2. Two views of combined detector model ( $\beta=5^\circ$ )

After applying the effect of  $C_{KN}$  and buildup factor to the conventional density formula, the final combined detector model equation will be as following:

$$\rho_{CDM} = C_1 \ln(I_{D1} - C_{KN} \times I_{D2}) + C_2 \quad (4)$$

3. Monte Carlo computations

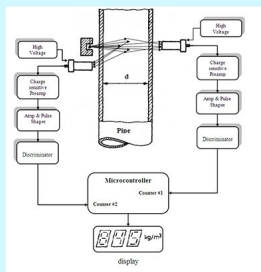
The required data for the intensity variation of gamma rays are computable with MCNP4C radiation transport code (Briesmeister, 2000; El Abd, 2014). Tally F8 was considered in our computations and the error for the whole simulation is approximately 0.0204. The MCNP will predict the number of photons reaching each detector. Then, by using equation (4), the density of each testing material could be calculated.

4. Experimental setup

The required data for the intensity variation of gamma rays are computable with MCNP4C radiation transport code (Briesmeister, 2000; El Abd, 2014). Tally F8 was considered in our computations and the error for the whole simulation is approximately 0.0204. The MCNP will predict the number of photons reaching each detector. Then, by using equation (4), the density of each testing material could be calculated.



Fig. 3. Transmission and backscatter CDM



5. Results and discussion

R square function plotted in figures (4) and (5) for CD model. Also comparison of conventional and combined detector model was done in Table 1. Results showed that the proposed correction of theoretical calculation represents a good estimation of the density and improves the linearity of the densitometry over conventional transmission technique. CDM, improved the measurement of density in experimental technique about 0.45% compared to the individually transmission measurement. Also, in simulation the CD model improved the R-square about 0.18%.

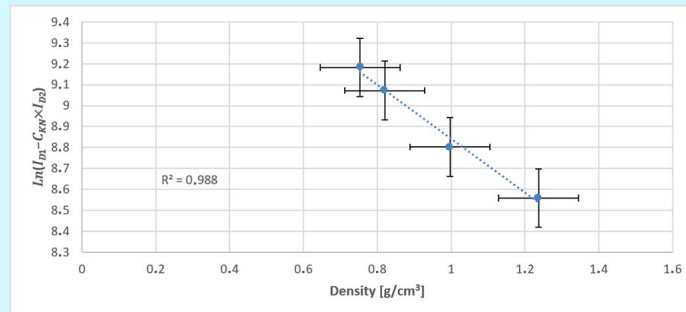


Fig. 4. Experimental CDM measurement for density of different materials

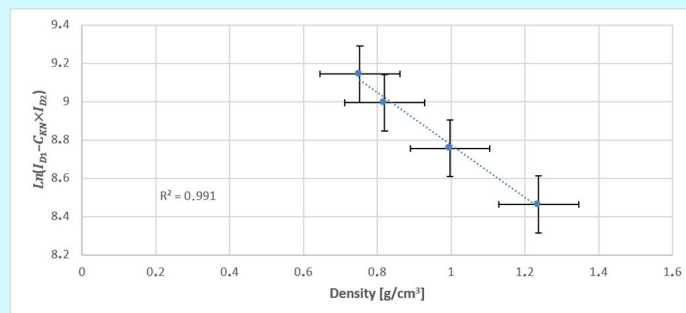


Fig. 5. MCNP calculation of CDM for density of different materials

Table 1. Total comparison between different density measurement methods

Method	R square
Combined detector model experimental measurement	0.988
Transmission experimental measurement	0.983
Combined detector model MCNP calculation	0.991
Transmission MCNP calculation	0.989

The CDM has remarkable advantages in comparison with the transmission technique. Computations introduced in this study of CDM showed that the application of two detectors in combination leads to decreased densitometry error and improved RSQ function of system. Furthermore, continuous calculation and monitoring of the buildup factor become possible. It was shown through computations that the need for the shield around the detector is resolved and the buildup factor could be obtained while using the data of both detectors (D1 and D2) in combination. In this study, the internal buildup reduction has been introduced and related formulation was deduced by specialized calculation. Hence, the combination of backscatter and transmission techniques for the measurement of the densities of fluids in the pipe is more efficient and precise than the traditional transmission technique. Also the MCNP4C simulation showed that the combined detector method is more efficient than transmission method.

References

Briesmeister, J., 2000. MCNP-A General Monte Carlo N-Particle Transport Code.  
 El Abd, A., 2014. Intercomparison of gamma ray scattering and transmission techniques for gas volume fraction measurements in two phase pipe flow. Nucl. Instrum. Meth. Phys. Res. A 735, 260-266.  
 Golgoun, S. M., Sardari, D., Sadeghi, M., Ebrahimi, M., Aminipour, M., Davarpanah, M. R. 2015. Combined backscatter and transmission method for nuclear density gauge. Eur. Phys. J. Web of Conferences 100, 02004.  
 Hasan, A. H. A. M., Lucas, G.P., 2011. Experimental and theoretical study of the gas-water two phase flow through a conductance multiphase Venturi meter in vertical annular (wet gas) flow. NUCL. ENG. DES. 241, 1998-2005.  
 He, D., Bai, B., 2014. A new correlation for wet gas flow rate measurement with Venturi meter based on two-phase mass flow coefficient. Measurement 58, 61-67.  
 IAEA-TECDOC-1459, 2005.  
 Johansen, G. A., Jackson, P., 2004. Radioisotope Gauges for Industrial Process Measurements, John Wiley & Sons.  
 Knoll, G.F., 2000. Radiation Detection and Measurement, 3<sup>rd</sup> ed. Wiley, New York.  
 Sowerby, B.D., Rogers, C.A. 2005. Appl. Radiat. Isotopes 63, 789.  
 Tan, S. A., Fwa, T. F., 1991. NDT & E INT. 24.  
 Thorn, R., Johansen, G. A., Hammer, E. A., 1997. Recent developments in three-phase flow measurement. Meas. Sci. Technol. 8, 691-701.

## Application of Monte Carlo simulations to waste management: projection for the DSRSs management in low income countries

**Authors:** Cebastien Joel GUEMBOU SHOUOP <sup>a, b, c, \*</sup>

<sup>a</sup> *UFD Mathématiques, Informatique Appliquée et Physique Fondamentale, Université de Douala, P.O. Box 24157, Douala, Cameroun*

<sup>b</sup> *National Radiation Protection Agency of Cameroon, Box 33732, Yaounde, Cameroon*

<sup>\*</sup>Corresponding author: [sebastianguembou@gmail.com](mailto:sebastianguembou@gmail.com)

### Abstract

The Management of Radioactive waste, generated from nuclear applications, has become a worldwide issue like the nuclear waste itself is a dam of several radionuclides with different half-lives, activities, and characteristics. The only well-used solution up-to-date is the long-term storage and disposal after its status of “waste” is confirmed. To be properly managed according to the regulations in place, Radioactive waste should be characterized and the appropriate geometries should be used for its disposal or long-term storage. This chapter describes the extension of the use of Monte Carlo simulation to properly manage radioactive waste, mainly in developing countries with low incomes. It thus deals with disused sealed radioactive sources (DSRS). Some applications to neutron and gamma disused sealed radioactive sources are highlighted as case studies. Since Monte Carlo methods are used to simulate the transport of particles, especially photon, electron, and neutron through matter and to obtain the detection system response, it is appropriate to be used during the research and development phase, while the DSRSs are under use before their disuse and classification as radioactive waste. The Particle and Heavy Ion Transport code System (PHITS) was used to perform the Monte Carlo simulation in the present work and the result of the GEANT4, FLUKA, and MCNP are to follow. The main outcomes are waste package geometry optimization-related.

**Keywords:** Monte Carlo; <sup>241</sup>Am/Be; DSRS; Neutron source; Radioactive waste; PHITS

### References:

Cebastien Joel GUEMBOU SHOUOP, Maurice NDONTCHUENG MOYO, Eric Jilbert NGUELEM MEKONGTSO et al. (2021 in press) 241AM/BE SOURCE OPTIMUM GEOMETRY FOR DSRSS MANAGEMENT-BASED MONTE CARLO SIMULATIONS. AIP Advances 11, 000000 (2021) <https://doi.org/10.1063/5.0063005>

# Standardization of Nuclear Data for the Production of Medical Radionuclides

The radionuclides produced at cyclotrons have achieved a significant place in medical science. The use of diagnostic and therapeutic radionuclides is now very common in many developed and some developing countries. The demand of new radionuclides is ever increasing and the search for the production of new potential radionuclides is necessary. The availability of experimental data and other databases of the IAEA are highlighted in this work. At Government College University in Lahore (Pakistan) a small group is continuously working for the standardization of nuclear data for the last 15 years. During the last few years we have developed a method for the standardization of the reaction cross sections to produce some emerging radionuclides of medical importance. The approach has been successfully applied for some radionuclides in a coordinated project of the IAEA. Nuclear model calculations are done using TALYS, EMPIRE, ALICE-IPPE for the production cross sections. In addition to study the core nuclear reactions for the production of some radionuclides; we have extensively focused on the calculation of impurities, yields and the energies. The evaluation entails nuclear-theory assisted statistical approach. A comparison of production routes are given along with the optimum energy range for the production of each radionuclide. The methodology is explained with the example of Y-86.

## Application Radiation

Radioactivity is a part of our earth - it has existed all along. Naturally occurring radioactive materials are present in its crust, the floors and walls of our homes, schools, or offices and in the food we eat and drink. There are radioactive gases in the air we breathe. Our own bodies - muscles, bones, and tissue - contain naturally occurring radioactive elements. Man has always been exposed to natural radiation arising from the earth as well as from outside the earth. The radiation we receive from outer space is called cosmic radiation or cosmic rays. We also receive exposure from man-made radiation, such as X-rays, radiation used to diagnose diseases and for cancer therapy. Fallout from nuclear explosives testing, and small quantities of radioactive materials released to the environment from coal and nuclear power plants, are also sources of radiation exposure to man. Radioactivity is the term used to describe disintegration of atoms. The atom can be characterized by the number of protons in the nucleus. Some natural elements are unstable. Therefore, their nuclei disintegrate or decay, thus releasing energy in the form of radiation. This physical phenomenon is called radioactivity and the radioactive atoms are called nuclei. The radioactive decay is expressed in units called becquerels. One becquerel equals one disintegration per second.

# Advanced Fuel Cycle Technique Development

With today's concerns about worldwide energy security and environmental impact nuclear power shows a unique potential as a large-scale sustainable energy source. However, despite the demonstrable safety record in nuclear technology high-level radioactive waste management remains a huge concern of nuclear fuel cycle long-term sustainability. Therefore, researchers proposed Advanced Fuel Cycle Initiative as an alternative method to high-level nuclear waste disposal in the future. This essay provides the fuel cycles development and the separations technologies to reduce spent fuel volume, separate long-lived, highly toxic elements, and reclaim spent fuel's valuable energy.

## Macroscopic and microscopic changes in borosilicate glasses after irradiation.

Borosilicate glasses are widely used to solidify the high level radioactive waste (HLW). It is accepted by many countries that borosilicate glasses should be treated with deep geological disposal. Suffering radiation from HLW, the stability of the borosilicate glasses is one of key points during long time disposal. With experimental simulation of radiation, one can predict how the stability of borosilicate glasses evolve with storage time or irradiation dose. In this work, borosilicate glasses were irradiated with ions and gamma rays to simulate radiation effects from alpha and gamma decays in vitrifications. The influence of radiation on macroscopic and microscopic properties of borosilicate glasses were studied. The different experimental methods are explained in detail, so as the experimental device. Results show different interacting mechanism from ions and gamma rays on the borosilicate glasses.

## Radioactive waste management for different state of radioactive waste

The demand of energy in current generation additionally carbon free energy is very high and it cannot be fulfilled by fossil fuels. At present, a large group of scientists are working on alternative to renewable energy in place of fossil fuels based energy. Renewable energy can fulfill our requirement and also give a better climate. Of all the renewable energy, nuclear energy is the most reliable solution to a fulfill energy demand and zero carbon emissions. The most important challenge with respect to nuclear energy is radioactive waste management technology development. The nuclear energy waste is very little in amount in compare to other method of energy production but it has high impact on environment for a longer time. Therefore, it is required a special management for disposal, so that it does not have any impact on the present environment as well as in future. To manage the risk of radioactive waste, we must first understand the methods of production and types of nuclear waste which is coming from the nuclear reactor unit, fuel production unit, laboratory etc. There are several types/ states or stages of nuclear waste. According to the type, mainly radioactive waste is classified into three categories. 1. Gas Radioactive Waste (GRW), 2. Liquid Radioactive Waste (LRW) and, 3. Solid Radioactive Waste (GRW). The second category of radioactive waste is depended on the level of activity. 1. High level Radioactive Waste (HLRW), 2. Medium level Waste (MLRW) and, 3. Low level Radioactive Waste (LLRW).

## Screening Constant by Unit Nuclear Charge Applications to the $3s3p5(3P\ 0\ 2,1,0\ 3)\ np, 3s23p33d(P1\ 1\ 0)\ ns$ and $3s23p33d(D3,2,1\ 3\ 0)\ ns$ Rydberg Series of $Ca^{3+}$ Ion

Malick SOW<sup>1\*</sup>

<sup>1</sup> Atoms-Lasers Laboratory, Department of Physics, Faculty of Sciences and Technologies, University Cheikh Anta Diop, Dakar, Sénégal

\*Contacts: [malick711.sow@ucad.edu.sn](mailto:malick711.sow@ucad.edu.sn)

**Abstract:** In this presentation, energy positions of the  $3s3p\ 5(P\ 0\ 2,1,0\ 3)\ np, 3s\ 23p\ 33d(P1\ 1\ 0)\ ns$  and  $3s\ 23p\ 33d(D3,2,1\ 3\ 0)\ ns$ , Rydberg series from metastable state of  $Ca^{3+}$  ion are reported. Calculations are performed up to  $n = 20$  using the Screening Constant by Unit Nuclear Charge (SCUNC) [1]. The present results compared well with the experimental data of Ghassan A Alna'washi [2] which are the only available values

### Introduction

Study of interaction photon - ionized matter is of great important in connection with the understanding of physical processes taking place in astrophysical (fig.1) and laboratory (fig.2) plasmas.

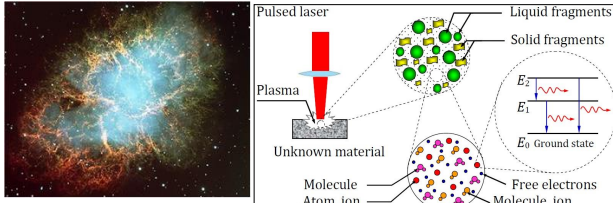


Fig 1. Astrophysical plasma.

Fig 2. Laboratory plasma created by laser.

Of great interest are Calcium atom and ions known to contribute to the opacity in the atmospheres of the central stars of planetary nebulas. The discovery of calcium-rich supernovae whose calcium nuclei represent (49%) of the ejected nuclei, i.e. five to ten times more than the number of calcium nuclei found in the thermonuclear supernovae and gravitational supernovae [3]. Also, absorption lines of neutral and ionized calcium are part of the characteristic spectral lines of many astrophysical systems including stars.

### Brief description of the SCUNC formalism

In the framework of the SCUNC formalism, the total energy of the  $(N\ell, n\ell')$   $2S+1L\pi$  excited states is expressed in the form (in Rydbergs)

$$E(N\ell, n\ell'; 2S+1L\pi) = -Z^2 \left( \frac{1}{N^2} + \frac{1}{n^2} \left[ 1 - \beta(N\ell, n\ell'; 2S+1L\pi; Z) \right] \right) \quad (1)$$

In this equation, the principal quantum numbers  $N$  and  $n$  are respectively for the inner and the outer electron of the helium-isoelectronic series. The  $\beta$ -parameters are screening constants by unit nuclear charge expanded in inverse powers of  $Z$  and given by [4]:

$$\beta(N\ell, n\ell'; 2S+1L\pi) = \sum_{k=1}^q f_k \left( \frac{1}{Z} \right)^k \quad (2)$$

Where  $f_k = f_k(2S+1L\pi; \mu, \nu, n, s)$  are screening constants to be evaluated empirically. In the photoionisation study, energy resonances are generally measured relatively to the  $E_{\infty}$  converging limit of a given  $(2S+1L\pi)n\ell'$ -Rydberg series. In Eq.(2),  $q$  stands for the number of terms in the expansion of the  $\beta$ -parameter. Generally, precise resonance energies are obtained for  $q < 5$ . The resonance energy are in the form:

$$E_n = E_{\infty} - \frac{Z^2}{n^2} \left\{ 1 - \frac{f_1(2S+1L\pi)}{Z(n-1)} - \frac{f_2(2S+1L\pi)}{Z} \pm \sum_{k=1}^q f_k^k F(n, \mu, \nu, s) \times \left( \frac{1}{Z} \right)^k \right\} \quad (3)$$

In this equation,  $\nu$  and  $\mu$  ( $\mu > \nu$ ) denote the principal quantum numbers of the  $(2S+1L\pi)n\ell'$  Rydberg series used in the empirical determination of the  $f_i$  - screening constants,  $s$  represents the spin of the  $n\ell'$ electron ( $s = 1/2$ ),  $E_{\infty}$  is the energy limit of the series,  $E_n$  denotes the resonance energy and  $Z$  stands for the atomic number.

The quantity  $\pm \sum_{k=1}^q f_k^k F(n, \mu, \nu, s) \times \left( \frac{1}{Z} \right)^k$  is a corrective term introduced to stabilize the resonance energies with increasing the principal quantum number  $n$ . In general, resonance energies are analyzed from the standard quantum-defect expansion formula.

$$E_n = E_{\infty} - \frac{RZ_{core}^2}{(n-\delta)^2}$$

### Resonance Energy of the $3s23p5(2P1/2) \rightarrow 3s3p5(3P2)np$ transitions of $Ca^{3+}$ :

Using Eq. (3), we find:

$$E_n = E_{\infty} - \frac{Z^2}{n^2} \left\{ 1 - \frac{f_1}{Z(n-1)} - \frac{f_2}{Z} + \frac{f_3}{Z} \times \frac{(n-\mu)(n-\nu)}{(n-\mu+s)(n-\nu-s)} + \frac{f_4}{Z} \times \frac{(n-\mu)(n-\nu)}{(n-\mu+\nu-3s)(n-\nu+2s)} \right\} \quad (4)$$

To evaluate the  $\beta$ -screening constant in Eq. (4), we use the ALS  $E_{exp}$  experimental data of Ghassan A. Alna'washi. [2]. From NIST [5] we get (in eV)  $E_{\infty} = 86.240$  eV. Thus for this transition, we get in eV [2]:

$$E_{\nu} = E_4 = 72.327 \pm 0.015 \quad (\nu=4) \text{ and } E_{\mu} = E_5 = 77.476 \pm 0.015 \quad (\mu=5)$$

respectively for the  $3s23p5(2P1/2) \rightarrow 3s3p5(3P2)4p$  and  $3s23p5(2P1/2) \rightarrow 3s3p5(3P2)5p$  transitions.

Using the Eq.(4), we find the empirical values of screening constants:

$$f_1 = -0.2194079 \pm 0.01453444 \quad ; \quad f_2 = 15.8818846 \pm 0.00702532$$

### Resonance Energy of the $3s23p5(2P1/2) \rightarrow 3s3p5(3P1)np$ transitions of $Ca^{3+}$ :

For this transition, using Eq. (3), we find:

$$E_n = E_{\infty} - \frac{Z^2}{n^2} \left\{ 1 - \frac{f_1}{Z(n-1)} - \frac{f_2}{Z} + \frac{f_3}{Z} \times \frac{(n-\mu)(n-\nu)}{(n-\mu+\nu+s)(n-\mu+\nu-s)} - \frac{f_4}{Z} \times \frac{(n-\mu)(n-\nu)}{(n-\mu+s)^2(n-\nu+s)} + \frac{f_5}{Z} \times \frac{(n-\mu)(n-\nu)(n-\mu-2s)}{(n-\mu-s)^2(n-\nu+s)^2} \right\} \quad (5)$$

To evaluate the  $\beta$ -screening constant in Eq. (5), we use the ALS  $E_{exp}$  experimental data of Ghassan A. Alna'washi. [2]. From NIST [5] we get (in eV)  $E_{\infty} = 86.640$  eV. Thus for this transition, we get in eV [2]:

$$E_{\nu} = E_4 = 72.773 \pm 0.015 \quad (\nu=4) \text{ and } E_{\mu} = E_5 = 77.816 \pm 0.015 \quad (\mu=5)$$

Using the Eq.(5), we find the empirical values of screening constants:

$$f_1 = -0.13910952 \pm 0.0148607 \quad ; \quad f_2 = 16.0080828 \pm 0.00713769$$

### Results and discussion

**Table 1:** Resonance energies  $E_n$ , quantum defects ( $\delta$ ) and effective charges ( $Z^*$ ) of the  $3s3p5(3P2)np$  Rydberg series from metastable state of  $Ca^{3+}$  ion. The present results (SCUNC) are expressed in eV and compared to the Advanced Light Source (ALS) data of Ghassan A. Alna'washi et al. [2].

n	$E_n$			$\delta$		$Z^*$
	SCUNC	ALS	$ \Delta E $	SCUNC	ALS	
4	72.327	72.327	0.000	0.04	0.04	4.045
5	77.255	77.255	0.000	0.08	0.07	4.043
6	80.093	80.089	0.004	0.04	0.05	4.028
7	81.743	81.741	0.003	0.06	0.04	4.023
8	82.775	82.772	0.003	0.08	0.08	4.019
9	83.496	83.493	0.003	0.10	0.10	4.014
10	84.011			0.12		4.008
11	84.395			0.14		4.005
12	84.688			0.16		4.003
13	84.916			0.18		4.003
14	85.097			0.20		4.002
15	85.244			0.22		4.002
16	85.364			0.24		4.002
17	85.463			0.26		4.002
18	85.547			0.28		4.001
19	85.618			0.30		4.001
20	85.678			0.32		4.001
$\infty$	86.240					

SCUNC: present results ; ALS [2].

**Table 2:** Resonance energies  $E_n$ , quantum defects ( $\delta$ ) and effective charges ( $Z^*$ ) of the  $3s3p5(3P1)np$  Rydberg series from metastable state of  $Ca^{3+}$  ion. The present results (SCUNC) are expressed in eV and compared to the Advanced Light Source (ALS) data of Ghassan A. Alna'washi et al. [2].

n	$E_n$			$\delta$		$Z^*$
	SCUNC	ALS	$ \Delta E $	SCUNC	ALS	
4	72.495	72.495	0.000	0.06	0.06	4.058
5	77.476	77.476	0.000	0.09	0.06	4.052
6	80.254	80.249	0.005	0.10	0.06	4.047
7	81.865	81.861	0.004	0.15	0.06	4.047
8	82.927	82.923	0.004	0.21	0.06	4.037
9	83.637	83.634	0.003	0.28	0.06	4.027
10	84.161			0.35		4.026
11	84.549			0.43		4.024
12	84.846			0.52		4.022
13	85.079			0.62		4.020
14	85.264			0.72		4.018
15	85.414			0.83		4.015
16	85.538			0.95		4.013
17	85.641			1.08		4.010
18	85.727			1.21		4.007
19	85.801			1.34		4.004
20	85.864			1.49		4.001
$\infty$	86.499					

SCUNC: present results ; ALS [2].

Overall, comparison shows that the SCUNC calculations agree well mainly with the ALS experimental data [2]. The precise data obtained from the SCUNC formalism is explained by the fact that the  $f_k$  - parameters [see Eq. (3)] are evaluated empirically using experimental data incorporating all relativistic and electron-electron effects. These relativistic and electron-electron effects are included implicitly in the [Eq.(4)].

**Acknowledgments:** The authors would like to thank gratefully acknowledgements the ICTP Organizing Committee. **References**

- [1]: M. T. Gning, Ibrahima Sakho, Malick Sow, J. of Modern. Phys., 11 (2020): 1891-1910.
- [2]: Ghassan A. Alna'washi et al. Phys. Rev. A 81(2010): 053416-053426.
- [3]: H.B. Perets et al. Int. J. Modern App. Physics. 2021, 11(1): 8-23
- [4]: Sakho, I., ISTE Science Publishing Ltd, London and John Wiley & Sons, Inc. USA. (2018).
- [5]: Ralchenko Y, Kramida NIST Atomic Spectra Database, MD, USA, (2016). <http://physics.nist.gov/asd33>